Interference in Exclusive Vector Meson Production in Heavy-Ion Collisions

Spencer R. Klein and Joakim Nystrand
Lawrence Berkeley National Laboratory, Berkeley, California 94720
(Received 3 September 1999)

Vector mesons are produced copiously in peripheral relativistic heavy-ion collisions. Virtual photons from one ion can fluctuate into quark-antiquark pairs and scatter from the second ion, emerging as vector mesons. The emitter and target are indistinguishable, so emission from the two ions will interfere. Vector mesons have negative parity so the interference is destructive, reducing the production of mesons with small transverse momentum. The mesons are short lived, and decay before emission from the two ions can overlap. However, the decay-product wave functions overlap and interfere since they are produced in an entangled state, providing an example of the Einstein-Podolsky-Rosen paradox.

PACS numbers: 25.75.Dw, 03.75.–b, 13.60.Le, 25.20.Lj

In relativistic heavy-ion collisions, vector mesons are copiously produced via photon-Pomeron fusion [1]. The photon and Pomeron both couple coherently to their emitting nuclei, giving these reactions a distinctive signature, with the final state consisting of the two nuclei, a vector meson with low perpendicular momentum ($p_\perp$) and nothing else. The latter requirement restricts these interactions to peripheral collisions, usually with impact parameter $b > 2R_A$, where R_A is the nuclear radius. At heavy-ion colliders, vector mesons with masses up to about $2\gamma\hbar c/R_A$, where γ is the Lorentz boost of each beam, are produced.

The electromagnetic field has a long range, while the nuclear (Pomeron) field has a short range compared to the size of the nucleus. So, vector meson production occurs in the region occupied by the Pomeron emitting ("target") nucleus. Since the production is coherent over the entire target nucleus, it is a fairly good approximation to treat the meson production regions as two point sources, one at the center of each nucleus. The situation is similar to that in a two-source interferometer, albeit with unstable particles. A parity inversion switches the emitter and target. Because of the vector meson negative parity, the two emission amplitudes have opposite sign. For perpendicular momentum $p_\perp \ll \hbar/b$, b being the impact parameter, the interference is destructive. We calculate here the magnitude of the interference and discuss the implications of the short vector meson lifetime, which causes the mesons to decay before wave functions from the two sources can overlap.

The cross sections for meson production can be calculated by convoluting the Weizsäcker-Williams virtual photon spectrum with the photonuclear interaction cross section. The photonuclear cross section is determined from data on γp interactions [2], using a Glauber formalism. In this approach, the photons are considered to fluctuate to virtual vector mesons, which then elastically scatter from the target nucleus, emerging as real mesons.

Earlier calculations summed the cross sections from the two nuclei and found very large rates [1]. Exclusive ρ^0 production was about 10% of the hadronic cross section for gold on gold collisions at a per nucleon center of mass energy $\sqrt{S_{NN}} = 200$ GeV as will be studied at the Relativistic Heavy Ion Collider (RHIC), rising to 50% for the $\sqrt{S_{NN}} = 5.5$ TeV lead on lead collisions at the Large Hadron Collider (LHC). The ω and ϕ production are about an order of magnitude smaller, while the J/ψ cross sections range from 0.3 mb (gold at RHIC) up to 32 mb (Pb at LHC). These cross sections correspond to production of hundreds of ρ^0 per second at RHIC, and hundreds of thousands of ρ^0 per second with calcium beams at the LHC. The J/ψ rates range from 0.06 Hz with gold at RHIC up to 780 Hz with calcium at LHC. These rates are comparable to those found at current and future meson factories.

For $p_\perp < \hbar/b$, it is impossible to tell which nucleus emitted the photon, and which elastically scattered the meson. So, the amplitudes are combined. Because vector mesons are negative parity, the two amplitudes subtract, rather than add, leading to destructive interference. In different terms, for $p_\perp b < \hbar$, a system of two identical nuclei has zero dipole moment, so radiation of vector particles is impossible. This is analogous to bremsstrahlung by identical particles [3], where there is destructive interference in the phase space where emission from the two particles overlaps. However, in contrast to bremsstrahlung photons, vector mesons are short lived, so that they decay before traveling far enough (the distance $|b|$) so that waves from the two production points can overlap. However, the decay product wave functions can overlap and do interfere.

The amplitude for vector meson production is $A(y, p_\perp, b)e^{i\phi(y)}$, with $A(y, p_\perp, b)$ the magnitude and $\phi(y)$ the phase at rapidity y. We assume that $A(y, p_\perp, b)e^{i\phi(y)}$ is symmetric with respect to rotations around the beam direction. The photon energy and perpendicular momentum are k and $k_\perp$, and the final meson momentum p. All values are in the center of mass frame, which corresponds to the laboratory frame for a heavy-ion collider. To eliminate the directional ambiguity, we adopt the convention that, for $y > 0$, the photon energy is higher than the Pomeron energy. Then, $A(y > 0) < A(y < 0)$ and $y = \ln(2k/M_V)$. Before discussing the total cross sections, we consider the final state perpendicular momentum.

 0031-9007/00/84(11)/2330(4)$15.00

The vector meson $p_\perp$ is the sum of the photon and Pomeron perpendicular momentum; these are the perpendicular momentum transfer from the photon emitter and target nuclei, respectively. The spectrum is a convolution of the two sources. The photon perpendicular momentum spectrum can be found with the equivalent photon approximation [4]

$$\frac{d^3N_\gamma(k,k_\perp)}{d^2k_\perp dk} = \frac{\alpha^2Z^2F^2(k_\perp^2 + k^2/\gamma^2)k_\perp^2}{\pi^2(k_\perp^2 + k^2/\gamma^2)^2}. \quad (1)$$

The nuclear form factor

$$F(q) = \frac{4\pi\rho_0}{Aq^3}[\sin(qR_A) - qR_A\cos(qR_A)]\left[\frac{1}{1 + a^2q^2}\right], \quad (2)$$

is the convolution of a hard sphere and a Yukawa potential with range $a = 0.7$ fm. This is an excellent fit to a Woods-Saxon density distribution [1]. Here, ρ_0 is the nuclear density and A the atomic number. For a given k, $k_\perp$ is independent of b, with $d^3N_\gamma(k,k_\perp)/d^2k_\perp dk$ rising from 0 at $k_\perp = 0$ to a maximum at $k_\perp = k/\gamma$ and then dropping as $k_\perp$ rises further.

Since the Pomeron range, <1 fm [5], is short, compared to the size of a nucleus, its perpendicular momentum spectrum is determined by Eq. (2). Figure 1 shows the photon and Pomeron perpendicular momentum spectra, along with their convolution, for $y = 0$ and $y = -2$. Diffractive dips are visible in the Pomeron spectrum; since the photon contribution to $p_\perp$ is usually small, these fringes also appear in the final $p_\perp$ spectrum. If the Pomeron had a longer range, the effect would be similar to increasing R_A; the $p_\perp$ spectrum would be shifted to lower values.

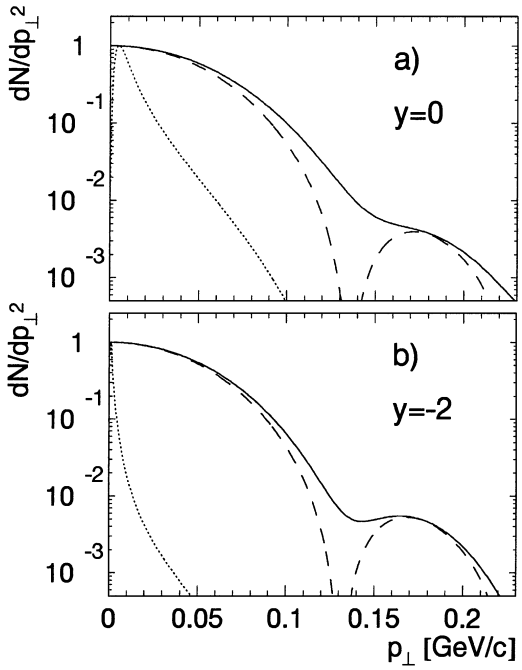

FIG. 1. Perpendicular momentum spectra for photons (dotted curves), Pomerons (dashed curves), and the final state vector mesons (solid curves) at (a) $y = 0$ and (b) $y = -2$ (corresponding to $k = 69$ MeV in the lab frame) for ϕ production in gold collisions at RHIC. The curves are each normalized to a maximum $dN/dp_\perp^2 = 1$. Clear diffraction minima appear in the Pomeron spectra. Since $k_\perp$ is small compared to $p_\perp$, the minima remain visible in the ϕ $p_\perp$ spectrum.

The impact parameter dependent photon energy spectrum was given in Ref. [1]. It was convoluted with $\sigma(\gamma A \to VA)$ to give $\sigma_{A+A\to A+A+V}(y,b)$. The nuclear photoproduction cross section was found with a Glauber calculation using $\sigma(\gamma p \to Vp)$ data as input. This calculation accounts for the effects of multiple interactions in the nucleus. The data are fit to $\sigma(\gamma p \to \gamma p) \sim XW^\epsilon + YW^{-\eta}$, where W is the γ-nucleon center of mass energy and ϵ, η, X, and Y are fit results [2]. The X,ϵ term represents Pomeron exchange, while Y,η is for photon-meson (primarily the f_0 [6]) fusion, present for the ρ and ω.

Since $p_\perp$ and b are conjugate variables, one cannot find a b-dependent photon $k_\perp$ spectrum; instead, we use the b-integrated $k_\perp$ spectrum, properly normalized, to find $\sigma_{A+A\to A+A+V}(y,p_\perp,b)$. Then, $A(y,p_\perp,b) = \sqrt{\sigma_{A+A\to A+A+V}(y,p_\perp,b)}$ where here both σ and A are for the photon coming from a known direction. So, this σ is half the total rate.

The production phase depends on the process. The soft Pomeron represents the absorptive part of the cross section, so the amplitude for photon-Pomeron fusion should be largely imaginary. There will be a small real part because the cross section rises slowly with photon energy, so $\phi(y) = \tan^{-1}(\pi\epsilon/4)$, independent of y [7]. For the light mesons, data indicate $\epsilon = 0.22$, so $\phi \sim 10^0$. For the J/ψ, $\epsilon = 0.8$, inconsistent with the soft Pomeron; the steep rise may be due to threshold behavior or signal the breakdown of the soft Pomeron model [8], but in either case, the J/ψ phase angle must be treated with caution. Of course, the phases for γA and γp reactions may be different.

For the ρ and ω, photon-meson fusion should have a different phase from the photon-Pomeron channel. Since $\eta > 1$, photon-meson fusion decreases as W rises; if the two channels have different phases, the overall phase will vary with y. Because the only available data are averaged over energy [9], we will ignore this variation. Of course, at $y = 0$, the energies are equal; as $|y|$ rises, any phase difference will grow.

For two nuclei at points $\vec{x}_1$ and $\vec{x}_2$, the amplitude A_0 for observing a vector meson at a distant point x_0 is found by approximating the vector mesons by plane waves. The meson momentum $\vec{p}$ is determined by $p_\perp$ and k via $p_\parallel = k - m_V^2/4k$. The amplitude is

$$A_0(x_0,\vec{p},b) = A(p_\perp,y,b)e^{i[\phi(y)+\vec{p}\cdot(\vec{x}_1-\vec{x}_0)]} - A(p_\perp,-y,b)e^{i[\phi(-y)+\vec{p}\cdot(\vec{x}_2-\vec{x}_0)]}. \quad (3)$$

The two components have opposite signs for rapidity because the photon emitters are coming from different directions. With the negative vector meson parity, this also gives the two components opposite signs.

The short-lived vector mesons will decay before reaching x_0. In fact, since the mean distance they travel before decaying, $\gamma\beta c\tau < b$, most will decay before their wave functions can overlap at all. However, their decay products can interfere, with $\vec{p}$ now being the sum of the daughter momenta. The resulting virtual interference pattern depends only on $\vec{p} \cdot \vec{b}$. The decay is incorporated by multiplying $A(p_\perp, y, b)$ by the decay amplitude, including the branching ratios, lifetime, and angular dependence. Since the angular distributions are the same for the two production directions, polarization does not affect the cross sections.

The decay products separate at relativistic velocities. For example, in $J/\psi \to e^+e^-$, the electron and positron are nearly back to back, and the e^+ (or e^-) amplitudes from the two sources cannot overlap each other until they are a good distance from their parent J/ψ. By the time the e^+ (and e^-) from the two sources overlap, the e^+ and e^- are well separated, and any interference involving both the e^+ and e^- requires a nonlocal wave function [10].

The decay product wave functions are entangled, with the form $\exp(ik_1x_1)\exp(ik_2x_1) - \exp(ik_2x_2)\exp(ik_2x_2)$, where k_1 and k_2 are the individual decay product momenta (for a two body decay), and cannot be factorized into individual particle wave functions. This interference is visible only by observing the complete final state. This nonlocal entanglement is an example of the Einstein-Podolsky-Rosen paradox [11]. However, the correlation depends on a continuous variable $p_\perp$, rather than more commonly considered discrete variables such as spin.

The individual decay products have much higher momenta than their parent meson, and could be used to reconstruct the meson decay point, and hence determine which nucleus emitted the meson. However, the position measurement would obscure their momentum enough to eliminate the interference pattern, as occurs with a two-slit interferometer [12].

In the center of mass frame, production is nearly simultaneous (within $\Delta t = b/c\gamma$), so time drops out. Since A is defined to be real,

$$\sigma(p_\perp, y, b) = A^2(p_\perp, y, b) + A^2(p_\perp, -y, b) - 2A(p_\perp, y, b)A(p_\perp, -y, b) \times \cos[\phi(y) - \phi(-y) + \vec{p} \cdot \vec{b}]. \quad (4)$$

At midrapidity, $y = 0$, the two source contributions are equal and the observed cross section is

$$\sigma(p_\perp, y = 0, b) = 2A^2(p_\perp, y = 0, b)(1 - \cos[\vec{p} \cdot \vec{b}]). \quad (5)$$

For a given b, σ oscillates with period $\Delta p_\perp = \hbar/b$. When $\vec{p} \cdot \vec{b} \ll 1$, the interference is destructive, and there is little emission.

Since b is in principle (but not in practice) measurable by examining the outgoing ions, it is an observable, and we integrate the cross section (not amplitude) over all possible b to get the total production. Figure 2 shows $d^2N/dp_\perp^2$ at $y = 0$ for gold and silicon beams at RHIC and calcium at LHC, with and without interference. The normalization here is arbitrary; the absolute cross sections are discussed in Ref. [1].

One could choose to measure the perpendicular momentum transfer from the two nuclei instead of b. Then, for $p_\perp > 10$ MeV/c, the larger momentum transfer will usually come from the target. This determination will break the symmetry, reducing the magnitude of the interference. Of course, near $p_\perp = 0$, the photon and Pomeron perpendicular momenta have very similar magnitudes, so the interference will remain. Because the initial nuclear momenta are not well known, it is not possible to determine which nucleus contributed the bulk of the $p_\perp$.

With gold beams at RHIC, vector meson production occurs with median impact parameters for ρ^0, ω, ϕ, and J/ψ production of 46, 46, 38, and 23 fm, respectively, corresponding to $p_\perp < 4$ MeV/c for the light mesons and $p_\perp < 10$ MeV/c for the J/ψ. Below these $p_\perp$ values, interference is large. With lighter nuclei, the average impact parameters are slightly smaller, leading to higher $p_\perp$ cutoffs. At the LHC, impact parameters are much larger, 170–290 fm for light vector mesons and 44–68 fm for the J/ψ, and the reduction is large only for quite small values of $p_\perp$.

Despite the dramatically different $p_\perp$ spectrum, the overall rate at $y = 0$ is unaffected by the interference. This is because $\langle p_\perp \rangle > \langle \hbar/b \rangle$, so the $\cos[\vec{p} \cdot \vec{b}]$ oscillations average out, leaving the rate almost unaffected.

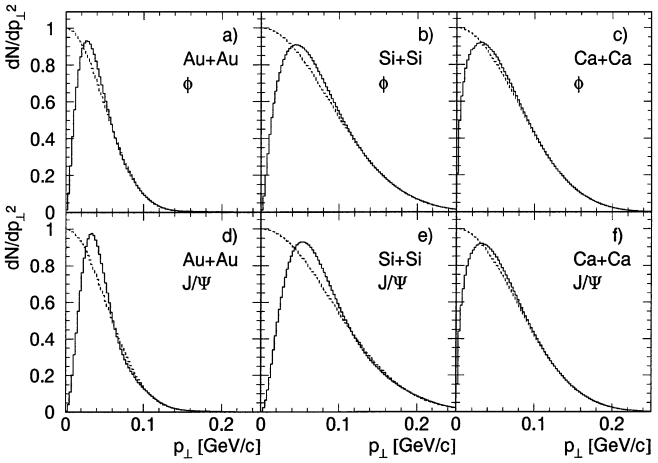

FIG. 2. Expected $p_\perp$ spectra for reconstructed ϕ and J/ψ mesons at $y = 0$ with (a),(d) gold beams at RHIC, (b),(e) silicon beams at RHIC, and (c),(f) calcium beams at LHC. The solid histograms include interference, while the dotted ones do not. Because of the smaller impact parameters production is peaked at higher $p_\perp$ in (b),(e) than in (a),(d). Because of the smaller impact parameters in (b),(e), the interference dip extends to higher $p_\perp$ than in (a),(d). In (c),(f), the energies are higher, leading to higher impact parameters, pushing the interference dip to lower $p_\perp$. The figure is normalized so that, without interference, $dN/dp_\perp^2 = 1$ at $p_\perp = 0$; the rates are given in Ref. [1].

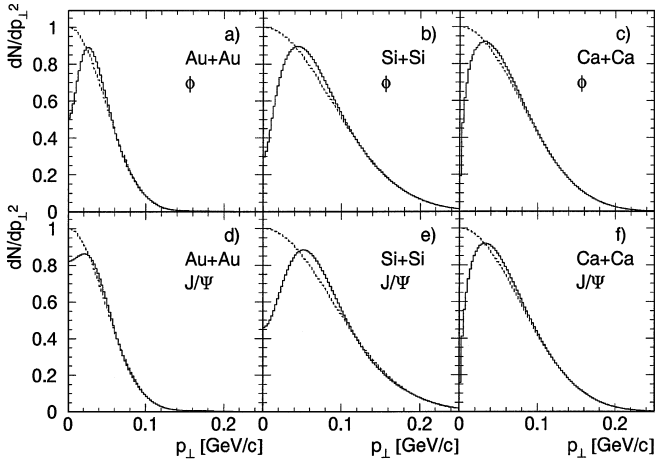

FIG. 3. Expected $p_\perp$ spectra for reconstructed ϕ and J/ψ mesons at $y = 1$ with (a),(d) gold beams at RHIC, (b),(e) silicon beams at RHIC, and (c),(f) calcium beams at LHC. The solid histograms include interference, while the dotted ones do not. Because of the difference in amplitudes, $dN/dp_\perp^2 \neq 0$ at $p_\perp = 0$. The size of the dip at $p_\perp = 0$ depends on the ratio of amplitudes at $y = 1$ and $y = -1$; it is larger for lighter nuclei and higher collision energies. This figure is normalized so that, without interference, $dN/dp_\perp^2 = 1$ at $p_\perp = 0$; the rates are given in Ref. [1].

Since the $p_\perp$ spectrum is almost independent of y, this remains true at other rapidities, so the total cross section is also unchanged.

Figure 3 shows $d^2N/dp_\perp^2$ at $y = 1$ for the same three cases. The magnitude of the interference is reduced because $A(y = 1) < A(y = -1)$. Without interference, the spectrum is slightly different because the photons have different energies, which leads to a slightly different $p_\perp$ spectrum.

This interference can be studied with the decays $\rho^0 \to \pi^+\pi^-$, $\omega \to \pi^+\pi^-$, $\phi \to K^+K^-$, and $J/\psi \to e^+e^-$, which are readily reconstructible. Because of the high rates, the backgrounds to these processes should be small; simulations indicate that this is indeed the case, at least for a large acceptance detector [13].

There are a few details that may slightly reduce the interference. Because the photon emission is electromagnetic, it is possible for the emitting nucleus to be excited into a giant dipole resonance (GDR); since the Pomeron is uncharged, excitation is unlikely for the scattering nucleus. However, even for the photon emitting nucleus, the excitation probability is relatively low. Excitation is much more likely if the nuclei exchange an additional photon between themselves, with equal excitation probabilities for both nuclei, and not affecting the interference [14]. Radiative corrections and other higher order processes could also reduce the interference. These factors should be small because the nuclear trajectories are barely affected by the interaction. Likewise, backgrounds from nonresonant (but coherent) photonuclear and two-photon processes should be small.

However, these backgrounds may introduce additional interference terms which may complicate the picture. For example, the process $\gamma\gamma \to e^+e^-$ can interfere with e^+e^- from J/ψ decays; the rate for the $\gamma\gamma \to e^+e^-$ to mimic J/ψ decays is small, but perhaps visible.

In conclusion, interference between emission between two colliding nuclei dramatically changes the perpendicular momentum spectrum of exclusively produced vector mesons, suppressing production of vector mesons at low $p_\perp$. Because the vector mesons decay before their wave functions can overlap, the interference involves all of the decay products, which never overlap with each other. So, the decay products have an entangled, nonlocal wave function.

We would like to acknowledge useful conversations with Stan Brodsky and Jørgen Randrup. This work was supported by the U.S. DOE, under Contract No. DE-AC-03-76SF00098.

[1] S. Klein and J. Nystrand, Phys. Rev. C **60**, 014903 (1999).
[2] These calculations are based on fits in J. A. Crittenden, *Exclusive Production of Neutral Vector Mesons at the Electron-Proton Collider HERA* (Springer-Verlag, Berlin, 1997). Similar, but slightly newer results appear in J. Breitweg *et al.*, Z. Phys. C **75**, 215 (1997); S. Aid *et al.*, Nucl. Phys. **B472**, 3 (1996).
[3] R. C. Stabler, Nature (London) **206**, 922 (1965).
[4] M. Vidovic, M. Greiner, C. Best, and G. Soff, Phys. Rev. C **47**, 2308 (1993); G. Baur and L. G. Ferreira Filho, Phys. Lett. B **254**, 30 (1991).
[5] B. Müller and A. J. Schramm, Nucl. Phys. **A523**, 677 (1991).
[6] D. Leith, in *Electromagnetic Interactions of Hadrons*, edited by A. Donnachie and G. Shaw (Plenum Press, New York, 1978), and references therein.
[7] J. R. Forshaw and D. A. Ross, *Quantum Chromodynamics and the Pomeron* (Cambridge University Press, Cambridge, England, 1997).
[8] N. Cartiglia, hep-ph/9703245, 1997.
[9] T. H. Bauer *et al.*, Rev. Mod. Phys. **50**, 261 (1978).
[10] M. A. Horne, A. Shimony, and A. Zeilinger, Phys. Rev. Lett. **62**, 2209 (1989).
[11] A. Einstein, B. Podolsky, and N. Rosen, Phys. Rev. **47**, 777 (1935).
[12] This situation is analogous to the two-slit interferometer described by T. Sudbery, in *Quantum Concepts in Space and Time*, edited by R. Penrose and C. J. Isham (Oxford, New York, 1986).
[13] J. Nystrand and S. Klein, in Proceedings of the Workshop on Photon Interactions and the Photon Structure, Lund, Sweden, 1998 (nucl-ex/9811007); S. Klein and J. Nystrand, STAR Note 347, 1998. Available on the web at http://www.star.bnl.gov/star/starlib/doc/www/sno/ice/sn0347.html.
[14] G. Baur, K. Hencken, and D. Trautman, J. Phys. G **24**, 1657 (1998).